

# Conformer Distribution in (*cis*-1,4-DACH)bis(guanosine-5'-phosphate)platinum(II) Adducts: A Reliable Model for DNA Adducts of Antitumoral Cisplatin

Rosa Ranaldo, Nicola Margiotta,\* Francesco P. Intini, Concetta Pacifico, and Giovanni Natile\*

Dipartimento Farmaco-Chimico, Università degli Studi di Bari, Via E. Orabona 4,  
70125 Bari, Italy

Received November 8, 2007

In  $[\text{PtCl}_2(\textit{cis}\text{-}1,4\text{-DACH})]$  (DACH = diaminocyclohexane), the N–Pt–N bite angle ( $\geq 97^\circ$ , as determined by X-ray diffraction analysis) is much larger than those found in other Pt complexes with bidentate diamines or in cisplatin ( $91^\circ$ ). Hence, the possibility exists that in  $(\textit{cis}\text{-}1,4\text{-DACH})\text{PtG}_2$  adducts, rotation of the G's around the Pt–N7 bonds is slowed enough to allow observation of different conformers. In accord with this prevision, decreasing the temperature to 238 K enabled us to observe different conformers of  $(\textit{cis}\text{-}1,4\text{-DACH})\text{Pt}(5'\text{-GMP})_2$  (GMP = guanosine monophosphate). This observation is the first case in which such conformers for a platinum derivative with primary diamines and untethered guanines have been resolved and represents the closest model to clinically effective cisplatin obtained to date. We also found that the presence of the 1,4-DACH ligand increased the intensity of the circular dichroism signal stemming from the dominance of an HT conformer ( $\Delta\text{HT}$  in the adduct with 3'-GMPs and  $\Delta\text{HT}$  in the adduct with 5'-GMPs).

## 1. Introduction

Cisplatin [*cis*-diamminedichloroplatinum(II), Figure 1] is one of the most active antitumor agents in clinical use.<sup>1</sup> However, it has a narrow spectrum of activity, and its clinical use is limited by undesirable side effects, including nephrotoxicity, ototoxicity, neurotoxicity, nausea, vomiting, and myelosuppression.<sup>2,3</sup> The search for new, more effective platinum drugs has led to second-generation [carboplatin, diammine(1,1-cyclobutanedicarboxylato(2-))-*O,O'*-platinum(II)]<sup>4</sup> and third-generation [oxaliplatin, ((1*R*,2*R*)-diaminocyclohexane)oxalatoplatinum(II)]<sup>5</sup> drugs, the latter of which is active against cisplatin-resistant tumors<sup>6</sup> and was approved for worldwide clinical use in 2004. Oxaliplatin contains 1,2-diaminocyclohexane [(1*R*,2*R*)-DACH] as the

\* To whom correspondence should be addressed. Phone: +39 080 5442774. Fax: +39 080 5442230. E-mail: natile@farmchim.uniba.it (G.N.), nmargiotta@farmchim.uniba.it (N.M.).

(1) *Cisplatin: Chemistry and Biochemistry of a Leading Anticancer Drug*; Lippert, B., Ed.; Wiley-VCH: Weinheim, Germany, 1999.

(2) Krakoff, I. H. In *Platinum and Other Metal Coordination Compounds in Cancer Chemotherapy: Clinical Applications of Platinum Complexes*; Nicolini, M., Ed.; Martinus Nijhoff Publishers: Boston, 1988; p 351.

(3) Wong, E.; Giandomenico, C. M. *Chem. Rev.* **1999**, 99, 2451.

(4) Harrap, K. R. *Cancer Treat. Rev.* **1985**, 12(Suppl. 1), 21.

(5) (a) Kidani, Y. *Trends Inorg. Chem.* **1990**, 1, 107. (b) Schmidt, W.; Chaney, S. *Cancer Res.* **1993**, 53, 799.

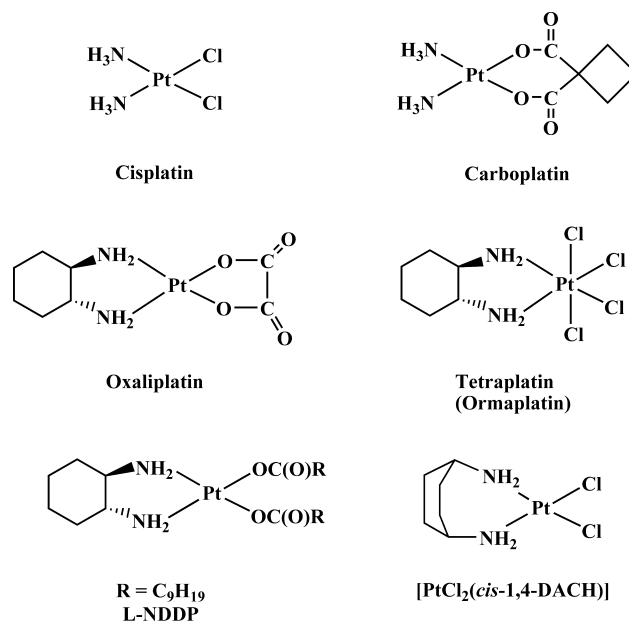
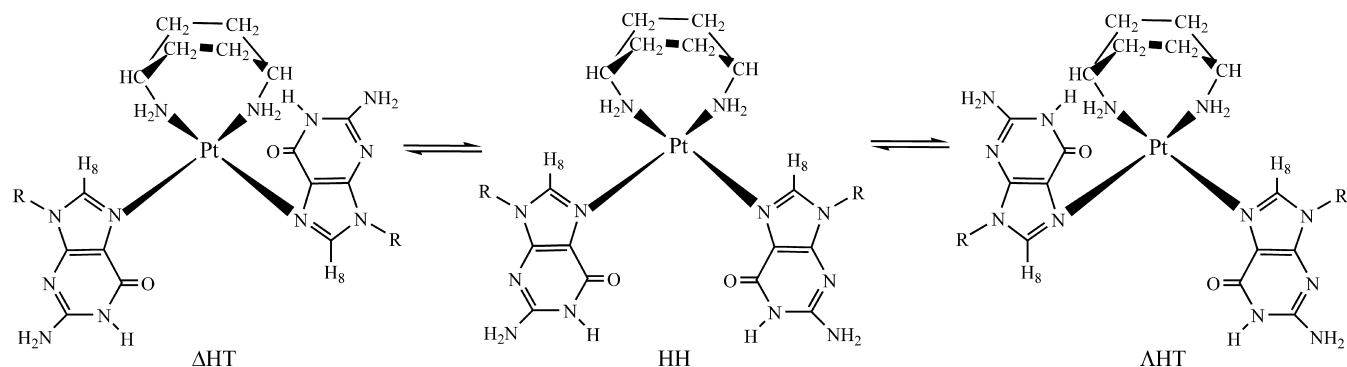


Figure 1. Chemical structures of platinum compounds.

carrier ligand, and the same ligand is found in ormaplatin [also called tetraplatin, ((1*R*,2*R*)-DACH)tetrachloroplatinum(IV)] and L-NDDP [(1*R*,2*R*)-DACH]bis(neodecanoato)-

**Scheme 1.** Sketch of (*cis*-1,4-DACH)PtG<sub>2</sub> Conformers (R = Ribose-5'-phosphate)

platinum(II)], which are currently in clinical trials. In addition, Pt compounds containing *cis*-1,4-diaminocyclohexane (*cis*-1,4-DACH) as the carrier ligand,<sup>7</sup> such as [PtCl<sub>2</sub>(*cis*-1,4-DACH)] (Figure 1), are being investigated.<sup>7b</sup> The latter compound has better activity than cisplatin in most cisplatin-resistant cell lines and is also active in oxaliplatin-resistant L1210 leukemia cells. In vivo experiments have also shown that [PtCl<sub>2</sub>(*cis*-1,4-DACH)] has better activity than cisplatin against platinum-resistant murine leukemias.

Since the discovery of cisplatin, many efforts have also been devoted to investigating its mechanism of action. It is now generally accepted that interaction with DNA (and its consequent distortion) is fundamental in triggering the cascade of events that leads to the death of tumor cells.<sup>8</sup> The major platinum–DNA adduct involves cross-linking of two adjacent guanines of the same strand (a 1,2-intrastrand cross-link).<sup>9</sup> Cisplatin can also cross-link guanine bases of opposite strands, forming an interstrand cross-link; however, this latter lesion is less common and is considered to be less important.<sup>10</sup>

Platinum compounds such as *cis*-A<sub>2</sub>PtG<sub>2</sub> [A<sub>2</sub> = two monodentate or one bidentate amine ligand, G<sub>2</sub> = two guanines that are either separate (untethered) or connected by a phosphodiester linkage] are the simplest models for Pt–DNA interactions, but even these simple models can have several conformations that differ in the relative orientations of the two guanine bases (Scheme 1). In the solid state of models containing untethered nucleotides, the six-membered rings of the two guanines are on opposite sides of the Pt coordination plane; this conformation is designated as head-

to-tail (HT, Scheme 1).<sup>11–13</sup> In only a few cases, such as in complexes containing 9-ethylguanine or 9-[(2-hydroxyethoxy)methyl]guanine (none containing nucleotides), has the head-to-head (HH) conformation been found in the solid state.<sup>11c,14</sup>

The HT conformation encompasses two different arrangements having different chiralities, which are defined as  $\Lambda$  and  $\Delta$  (Scheme 1). In solution, *cis*-A<sub>2</sub>PtG<sub>2</sub> complexes usually exhibit free rotation about the Pt–N7 bonds that precludes investigation of individual conformers.<sup>15</sup> Cramer was the first to demonstrate that guanosine rotation in *cis*-A<sub>2</sub>PtG<sub>2</sub> complexes with bulky A<sub>2</sub> ligand(s) (such as *N,N,N',N'*-tetramethylethylenediamine<sup>15a</sup>) can be slowed enough to permit detection of different conformers in solution.

The number of conformers at equilibrium depends upon the symmetry of the *cis*-A<sub>2</sub>Pt residue. In particular, diamine ligands having C<sub>2</sub> symmetry can have only one HH conformer and two HT conformers ( $\Lambda$  and  $\Delta$ ).<sup>16</sup>

The stability of different conformers is influenced by interactions between *cis* ligands (nucleotide–nucleotide and amine–nucleotide interactions). Nucleotide–nucleotide in-

- (6) Eastman, A.; Illenye, S. *Cancer Treat. Rep.* **1984**, 68, 1189. (b) Burchenal, J. H.; Kalaher, K.; Dew, K.; Lokys, L. *Cancer Treat. Rep.* **1979**, 63, 1493.
- (7) (a) Ali Khan, S. R.; Khokhar, A. R. *J. Coord. Chem.* **2000**, 51, 323. (b) Hoeschele, J. D.; Showalter, H. D. H.; Kraker, A. J.; Elliot, W. L.; Roberts, B. J.; Kampf, J. W. *J. Med. Chem.* **1994**, 37, 2630. (c) Khokhar, A. R.; Shamsuddin, S.; Xu, Q. *Inorg. Chim. Acta* **1994**, 219, 193. (d) Shamsuddin, S.; Khokhar, A. R. *J. Coord. Chem.* **1994**, 33, 83. (e) Shamsuddin, S.; Santillan, C. C.; Stark, J. L.; Whitmire, K. H.; Siddik, Z. H.; Khokhar, A. R. *J. Inorg. Biochem.* **1998**, 71, 29. (f) Shamsuddin, S.; Takahashi, I.; Siddik, Z. H.; Khokhar, A. R. *J. Inorg. Biochem.* **1996**, 61, 291.
- (8) Wang, D.; Lippard, S. *J. Nat. Rev. Drug Discovery* **2005**, 4, 307.
- (9) (a) Fichtinger-Schepman, A. M. J.; van der Veer, J. L.; den Hartog, J. H. J.; Lohman, P. H. M.; Reedijk, J. *Biochemistry* **1985**, 24, 707. (b) Eastman, A. *Biochemistry* **1986**, 25, 3912.
- (10) Pinto, A. L.; Lippard, S. *J. Biochim. Biophys. Acta* **1985**, 780, 167.

- (11) (a) Sherman, S. E.; Gibson, D.; Wang, A. H. J.; Lippard, S. *J. Science* **1985**, 230, 412. (b) Grabner, S.; Plavec, J.; Bukovec, N.; Leo, D. D.; Cini, R.; Natile, G. *J. Chem. Soc., Dalton Trans.* **1998**, 1447. (c) Bau, R.; Gellert, R. W. *Biochimie* **1978**, 60, 1040. (d) Lippert, B. *Prog. Inorg. Chem.* **1989**, 37, 1. (e) Schollhorn, H.; Raudaschl-Sieber, G.; Muller, G.; Thewalt, U.; Lippert, B. *J. Am. Chem. Soc.* **1985**, 107, 5932. (f) Sinur, A.; Grabner, S. *Acta Crystallogr., Sect. C* **1995**, 51, 1769.
- (12) (a) Marzilli, L. G.; Chalipoyil, P.; Chiang, C. C.; Kistenmacher, T. J. *J. Am. Chem. Soc.* **1980**, 102, 2480. (b) Barnham, K. J.; Bauer, C. J.; Djuran, M. J.; Mazid, M. A.; Rau, T.; Sadler, P. J. *Inorg. Chem.* **1995**, 34, 2826. (c) Kistenmacher, T. J.; Chiang, C. C.; Chalipoyil, P.; Marzilli, L. G. *J. Am. Chem. Soc.* **1979**, 101, 1143.
- (13) (a) Benedetti, M.; Tamasi, G.; Cini, R.; Natile, G. *Chem.—Eur. J.* **2003**, 9, 6122. (b) Benedetti, M.; Tamasi, G.; Cini, R.; Marzilli, L. G.; Natile, G. *Chem.—Eur. J.* **2007**, 13, 3131.
- (14) (a) Cini, R.; Grabner, S.; Bukovec, N.; Cerasino, L.; Natile, G. *Eur. J. Inorg. Chem.* **2000**, 1601. (b) Lippert, B.; Raudaschl, G.; Lock, C. J. L.; Pilon, P. *Inorg. Chim. Acta* **1984**, 93, 43.
- (15) (a) Cramer, R. E.; Dahlstrom, P. L. *J. Am. Chem. Soc.* **1979**, 101, 3679. (b) Cramer, R. E.; Dahlstrom, P. L. *Inorg. Chem.* **1985**, 24, 3420. (c) Cramer, R. E.; Dahlstrom, P. L.; Seu, M. J. T.; Norton, T.; Kashiwagi, M. *Inorg. Chem.* **1980**, 19, 148. (d) Dijt, F. J.; Canters, G. W.; Den Hartog, J. H. J.; Marcelis, A. T. M.; Reedijk, J. *J. Am. Chem. Soc.* **1984**, 106, 3644. (e) Marcelis, A. T. M.; Korte, H. J.; Krebs, B.; Reedijk, J. *Inorg. Chem.* **1982**, 21, 4059. (f) Marcelis, A. T. M.; van der Veer, J. L.; Zwetsloot, J. C. M.; Reedijk, J. *Inorg. Chim. Acta* **1983**, 78, 195. (g) Miller, S. K.; Marzilli, L. G. *Inorg. Chem.* **1985**, 24, 2421.
- (16) Natile, G.; Marzilli, L. G. *Coord. Chem. Rev.* **2006**, 250, 1315 and references therein.

teractions include the following: (1) Electrostatic attraction in HT conformers between the electron-rich O6 of one guanine and the electron-deficient H8 of the other (the “cis G”), both of which are on the same side of the platinum coordination plane. In these conformers, this interaction is generally responsible for causing the six-membered ring of each guanine to lean toward the cis G in order to bring the two oppositely charged moieties closer to each other (a “6-in” conformation). (2) Electrostatic repulsion in the HH conformer between the electron-rich O6's, both of which are located on the same side of the platinum coordination plane. This interaction generally leads to “6-out” canting of the guanines. (3) H bonding between the nucleotide phosphate of one G and N1H of the cis G. In the case of 5'-GMP (GMP = guanosine monophosphate), this interaction favors the  $\Delta$ HT conformer (since in  $\Delta$ HT, each *anti*-5'-GMP has the 5'-phosphate protruding toward the cis G), while in the case of 3'-GMP, it favors  $\Delta$ HT (since in  $\Delta$ HT, each *anti*-3'-GMP has the 3'-phosphate protruding toward the cis G).

Amine nucleotide interactions can also be of different types: (1) Steric interactions between the amine and the cis G. In HT conformers having the 6-in conformation, the relevant interaction involves the amine and H8 of the cis G, while in the HH conformer having the 6-out conformation, the relevant interaction involves the amine and the six-membered ring of the cis G. (2) H bonding between the amine NH (when present) and the 5'-phosphate of the cis G. For HT conformers with *anti*-5'-GMP, only  $\Delta$  chirality allows for such an interaction. (3) Finally, H bonding between the amine NH (when present) and O6 of the cis G. This interaction becomes significant after deprotonation of the guanine N1H at basic pH.

The  $A_2$  ligand selected for the present study (*cis*-1,4-DACH), when bound to platinum, forms a seven-membered chelate ring, which is much larger than the usual five- or six-membered rings. This results in a very large bite angle of  $\geq 97^\circ$ ,<sup>7,17,18</sup> which is much larger than those usually found in platinum complexes involving other diamines or even two cis ammines {e.g.,  $93^\circ$  in  $[\text{PtCl}_2(\text{pn})]$  (pn = 1,3-propanediamine),<sup>19</sup>  $91^\circ$  in cisplatin,<sup>20</sup> and  $83^\circ$  in  $[\text{PtCl}_2(\text{en})]$  (en = ethylenediamine)<sup>21</sup>}. Such a large angle could have the effect of increasing the steric interactions between cis guanines in *cis*- $A_2\text{PtG}_2$  adducts, thereby slowing the rotation of the G's about the Pt–N7 bonds and reducing the rate of interconversion between possible conformers. Furthermore, the N–Pt–N bite angles in pn, en, and *cis*-diammine derivatives were found to modulate the intensity of the circular dichroism (CD) band stemming from dominance of one HT conformer, particularly in adducts with 5'-GMP.<sup>13b</sup> Therefore, the (*cis*-1,4-DACH) $\text{PtG}_2$  system appeared to be worth investigating,

since it could allow observation of individual conformers in an adduct involving a primary diamine, the closest model to clinically relevant cisplatin.

It is also worth mentioning that, according to Hoeschele's results,<sup>7b</sup>  $[\text{PtCl}_2(\text{cis-1,4-DACH})]$  was more effective than cisplatin and oxaliplatin in several *in vivo* and *in vitro* tests. It is possible that differences in the conformations of its adducts with DNA could play a role in eliciting the enhanced antitumor activity.

## 2. Experimental Section

**2.1. Materials and Methods.** 5'-Guanosine monophosphate and 3'-guanosine monophosphate (Sigma) were used as received.

The *cis*-1,4-DACH ligand was synthesized according to a previously described procedure,<sup>22</sup> while *cis*- $[\text{Pt}(\text{dmsO})_2\text{Cl}_2]$  (dmsO = dimethyl sulfoxide) was prepared according to the method of Kukushkin.<sup>23</sup>

<sup>1</sup>H NMR spectra were recorded on Bruker Avance DPX 300 MHz and Avance II 600 MHz instruments. Chemical shifts ( $\delta$ ) are given in parts per million and referenced to the internal standard sodium 3-(trimethylsilyl)propionate (TSP). <sup>1</sup>H NMR experiments at different temperatures were performed using the heating control unit of the spectrometer equipped with a liquid-nitrogen apparatus. CD and UV–vis spectra were recorded on a Jasco J-810 spectropolarimeter at room temperature over the wavelength range 200–350 nm. The scan rate was 50 nm/min, and data were sampled every 0.1 nm. Each spectrum was averaged over 16 different scans in order to increase the signal-to-noise ratio. The path length of the cell was 0.5 cm. Concentrations were measured from the absorbance at 260 nm using an extinction coefficient of  $11.5 \text{ L mmol}^{-1} \text{ cm}^{-1}$ .<sup>24</sup>

A Crison Micro-pH meter (model 2002) equipped with Crison standard buffer solutions at pH 4.01, 7.02, and 9.26 was used for pH measurements. Values of pH for D<sub>2</sub>O solutions are indicated as pH\* values and were not corrected for the effect of deuterium on the glass electrodes.<sup>25</sup>

Liquid chromatography–electrospray ionization mass spectrometry (LC–ESI-MS) analyses were performed on an Agilent 1100 Series LC/MSD Trap System VL.

**2.2. Synthesis of the Complexes.** **2.2.1.  $[\text{PtCl}_2(\text{cis-1,4-DACH})]$ .**  $[\text{PtCl}_2(\text{cis-1,4-DACH})]$  was prepared following the procedure reported by Khokhar and co-workers<sup>26</sup> with slight modifications. The first step of this procedure involves the preparation of  $[\text{Pt}(\text{CBDCA})(\text{cis-1,4-DACH})]$  (CBDCA = 1,1-cyclobutanedicarboxylate), which subsequently is converted into the dichloro complex.

CBDCA (976 mg, 6.77 mmol) was dissolved in water (130 mL) and neutralized with Ag<sub>2</sub>O (1.57 g, 6.77 mmol). After the dicarboxylate solution was stirred in the dark at room temperature for 20 min, it was treated with *cis*- $[\text{PtCl}_2(\text{dmsO})_2]$  (2.86 g, 6.77 mmol); the resulting suspension was stirred for 10 min at 70 °C and then for 24 h at room temperature in the dark. The suspension was filtered to separate the AgCl precipitate, and the resulting solution was concentrated to 30 mL under reduced pressure and then kept at 0 °C for a few hours, during which a white crystalline

(17) Shamsuddin, S.; Ali, M. S.; Whitmire, K. H.; Khokhar, A. R. *Polyhedron* **2007**, *26*, 637.

(18) Shamsuddin, S.; van Hal, J. W.; Stark, J. L.; Whitmire, K. H.; Khokhar, A. R. *Inorg. Chem.* **1997**, *36*, 5969.

(19) Odoko, M.; Okabe, N. *Acta Crystallogr., Sect. C* **2006**, *62*, m136.

(20) Raudaschl, G.; Lippert, B.; Hoeschele, J. D.; Howard-Lock, H. E.; Lock, C. J. L.; Pilon, P. *Inorg. Chim. Acta* **1985**, *106*, 141.

(21) Ellis, L. T.; Hambley, T. W. *Acta Crystallogr., Sect. C* **1994**, *50*, 1888.

(22) Johnston, T. P.; McCaleb, G. S.; Clayton, S. D.; Frye, J. L.; Krauth, C. A.; Montgomery, J. A. *J. Med. Chem.* **1977**, *20*, 279.

(23) Kukushkin, Y. N.; Vyaz'menkii, Y. E.; Zorina, L. I.; Pazukhina, Y. L. *Zh. Neorg. Khim.* **1968**, *13*, 1595.

(24) *CRC Handbook of Biochemistry and Molecular Biology*, 3rd ed.; CRC Press: Cleveland, OH, 1975; Vol. I.

(25) Feltham, R. D.; Hayter, R. G. *J. Chem. Soc.* **1964**, 4587.

(26) Shamsuddin, S.; Takahashi, I.; Siddik, Z. H.; Khokhar, A. R. *J. Inorg. Biochem.* **1996**, *61*, 291.



**Table 1.**  $^1\text{H}$  and  $^{195}\text{Pt}$  Chemical Shifts (ppm) for  $[\text{PtCl}_2(\text{cis-1,4-DACH})]$  in Various Solvents<sup>a</sup>

| solvent                        | $^1\text{H}$ NMR                           |   |                |                   | $^{195}\text{Pt}$ NMR |
|--------------------------------|--|---|----------------|-------------------|-----------------------|
|                                | $\text{NH}_2$                              | $\text{H}_a^b$                              | $\text{H}_b^c$ | $\text{H}_{b'}^c$ |                       |
| DMF- <i>d</i> <sub>7</sub>     | 5.12 (s)<br>( $^2J_{\text{Pt-H}} = 77$ Hz) | 3.43 (s)<br>( $^3J_{\text{Pt-H}} = 94$ Hz)  | 2.11–2.03 (br) | 1.84–1.77 (br)    | –2212                 |
| dmsO- <i>d</i> <sub>6</sub>    | 4.90 (s)<br>( $^2J_{\text{Pt-H}} = 70$ Hz) | 2.95 (s)<br>( $^3J_{\text{Pt-H}} = 90$ Hz)  | 1.73–1.66 (br) | 1.48–1.43 (br)    | –2197                 |
| acetone- <i>d</i> <sub>6</sub> | 4.52 (s)<br>( $^2J_{\text{Pt-H}} = 80$ Hz) | 3.43 (s)<br>( $^3J_{\text{Pt-H}} = 96$ Hz)  | 2.00–1.97 (br) | 1.76–1.72 (br)    | –                     |
| D <sub>2</sub> O               | 4.91 (s)                                   | 3.19 (s)<br>( $^3J_{\text{Pt-H}} = 104$ Hz) | 1.74–1.73 (br) | 1.74–1.73 (br)    | –                     |
| CDCl <sub>3</sub>              | 4.76 (s)                                   | 3.34 (s)<br>( $^3J_{\text{Pt-H}} = 92$ Hz)  | 2.20–2.10 (br) | 1.70–1.66 (br)    | –                     |

<sup>a</sup> Abbreviations: s = singlet (with satellites when  $J_{\text{Pt-H}}$  are reported); br = broad. <sup>b</sup>  $\text{H}_a$  designates the protons on the tertiary carbon atoms. <sup>c</sup>  $\text{H}_b$  and  $\text{H}_{b'}$  designate the protons on the secondary carbon atoms. One geminal proton ( $\text{H}_b$ ) points outward from the cyclohexane ring, while the other proton ( $\text{H}_{b'}$ ) points inward toward the center of the cyclohexane ring.

solid of  $\text{cis-}[\text{Pt}(\text{CBDCA})(\text{dmsO})_2]$  precipitated from solution. The solid was isolated by filtration of the mother liquor, washed with cold water, and dried in vacuo (1.77 g, 3.59 mmol, 53% yield). Anal. Calcd for  $[\text{Pt}(\text{CBDCA})(\text{dmsO})_2]$  ( $\text{C}_{10}\text{H}_{18}\text{O}_6\text{S}_2\text{Pt}$ ): C, 24.34; H, 3.68. Found: C, 23.40; H, 3.88.  $^1\text{H}$  NMR (ppm, D<sub>2</sub>O): 3.58 (s, 3H), 2.80 (t,  $^3J_{\text{H-H}} = 7.90$  Hz, 4H), 1.94 (quintet,  $^3J_{\text{H-H}} = 7.90$  Hz, 2H). ESI-MS:  $m/z$  516  $[\text{M} + \text{Na}]^+$ .

$\text{cis-}[\text{Pt}(\text{CBDCA})(\text{dmsO})_2]$  (1.77 g, 3.59 mmol) was dissolved in water (150 mL) and treated with a solution of  $\text{cis-1,4-DACH}$  (0.67 g, 3.59 mmol) in Et<sub>2</sub>O (obtained by extraction with Et<sub>2</sub>O of an aqueous solution of  $\text{cis-1,4-DACH} \cdot 2\text{HCl}$  treated with excess NaOH). The volatile organic solvent was removed by distillation under reduced pressure, and the resulting aqueous solution was stirred at 90 °C for 1.5 h. The filtered hot solution was allowed to cool to room temperature, concentrated to 30 mL under reduced pressure, and kept at 0 °C for a few hours. The off-white precipitate of  $[\text{Pt}(\text{CBDCA})(\text{cis-1,4-DACH})]$  (0.53 g, 1.17 mmol, 32% yield) was recovered by filtration of the mother liquor followed by recrystallization from water. Anal. Calcd for  $[\text{Pt}(\text{CBDCA})(\text{cis-1,4-DACH})] \cdot \text{H}_2\text{O}$  ( $\text{C}_{12}\text{H}_{22}\text{O}_5\text{N}_2\text{Pt}$ ): C, 30.70; H, 4.72; N, 5.97. Found: C, 30.23; H, 4.78; N, 5.86.  $^1\text{H}$  NMR (ppm, D<sub>2</sub>O): 3.16 (pseudotriplet,  $^3J_{\text{Pt-H}} = 100.83$  Hz, 2H), 2.89 (t,  $^3J_{\text{H-H}} = 7.90$  Hz, 4H), 1.90 (quintet,  $^3J_{\text{H-H}} = 7.90$  Hz, 2H), 1.76 (s, 8H). ESI-MS:  $m/z$  450  $[\text{M} - \text{H}]^-$ .

$[\text{Pt}(\text{CBDCA})(\text{cis-1,4-DACH})]$  (0.43 g, 0.96 mmol) was suspended in 50 mL of concentrated HCl (37 wt %) and stirred for 2 days at room temperature. The yellow solution thereby obtained was dried to completion by evaporation of the solvent under reduced pressure, and the yellow residue was washed with cold water and dried under vacuum. This yielded a yellow crystalline product that proved to be  $[\text{PtCl}_2(\text{cis-1,4-DACH})]$  (0.239 g, 0.63 mmol, 66% yield referred to platinum). Anal. Calcd for  $[\text{PtCl}_2(\text{cis-1,4-DACH})]$  ( $\text{C}_6\text{H}_{14}\text{Cl}_2\text{N}_2\text{Pt}$ ): C, 18.96; H, 3.71; N, 7.37. Found: C, 18.85; H, 3.72; N, 7.29. ESI-MS:  $m/z$  402  $[\text{M} + \text{Na}]^+$ .  $^1\text{H}$  and  $^{195}\text{Pt}$  chemical shifts for  $[\text{PtCl}_2(\text{cis-1,4-DACH})]$  in various solvents are reported in Table 1. Crystals of  $[\text{PtCl}_2(\text{cis-1,4-DACH})]$  suitable for single-crystal X-ray investigation were obtained from a dimethylformamide (DMF) solution layered under diethyl ether.

**2.2.2.  $[\text{Pt}(\text{OSO}_3)(\text{cis-1,4-DACH})(\text{OH}_2)]$ .**  $[\text{PtCl}_2(\text{cis-1,4-DACH})]$  (60 mg, 0.16 mmol) was suspended in 15 mL of H<sub>2</sub>O, and the solution was treated with Ag<sub>2</sub>SO<sub>4</sub> (50 mg, 0.16 mmol) and stirred at room temperature for 24 h. The suspension was filtered through Celite in order to remove AgCl, and the solvent was evaporated to dryness under reduced pressure, yielding the desired compound  $[\text{Pt}(\text{OSO}_3)(\text{cis-1,4-DACH})(\text{OH}_2)]$  (66 mg, 0.15 mmol, 94% yield referred to platinum) as a white residue. Anal. Calcd for  $[\text{Pt}(\text{OSO}_3)(\text{cis-1,4-DACH})(\text{OH}_2)] \cdot \text{H}_2\text{O}$  ( $\text{C}_6\text{H}_{18}\text{O}_6\text{N}_2\text{S}_2\text{Pt}$ ): C, 16.33; H, 4.11; N,

6.35. Found: C, 16.50; H, 4.04; N, 6.33.  $^1\text{H}$  NMR (ppm, D<sub>2</sub>O): 5.41 (br, 2H), 5.28 (br, 2H), 3.05 (pseudotriplet,  $^3J_{\text{Pt-H}} = 109.58$  Hz, 2H), 1.77 (s, 8H).

**2.2.3.  $(\text{cis-1,4-DACH})\text{PtG}_2$  Adducts ( $\text{G} = 3'\text{-GMP}, 5'\text{-GMP}$ ).** A solution of G (0.025 mmol) and  $[\text{Pt}(\text{OSO}_3)(\text{cis-1,4-DACH})(\text{OH}_2)]$  (0.012 mmol) in 1 mL of D<sub>2</sub>O was adjusted with D<sub>2</sub>SO<sub>4</sub> to pH\* ~3 and transferred into an NMR tube. The concentration of the platinum complex was 10 mM. The progress of the reaction was monitored by  $^1\text{H}$  NMR spectroscopy.

**2.3. Solutions for CD Spectroscopy.** Aliquots (6  $\mu\text{L}$ ) of the  $(\text{cis-1,4-DACH})\text{PtG}_2$  solutions used in the NMR investigations (10 mM) were diluted by addition to an aqueous solution of Na<sub>2</sub>SO<sub>4</sub> (1.2 mL, 50 mM; the salt was required in order to maintain a constant ionic strength) in order to obtain a final complex concentration of  $4\text{--}5 \times 10^{-5}$  M. The pH of the solution was adjusted to values in the range 3–11 by addition of H<sub>2</sub>SO<sub>4</sub> ( $1.2 \times 10^{-2}$  M) or NaOH ( $2.5 \times 10^{-2}$  M).

**2.4. Crystallographic Measurements.** A yellow, needle-shaped crystal of  $[\text{PtCl}_2(\text{cis-1,4-DACH})] \cdot \text{DMF}$  was selected at the microscope and mounted on a glass fiber. The diffraction data were collected using a Bruker AXS X8 APEX CCD system equipped with a four-circle Kappa goniometer and a 4K CCD detector with Mo K $\alpha$  radiation ( $\lambda = 0.71073$  Å). The full data set was collected at  $293 \pm 2$  K. The number of measured reflections was 27693, and the number of independent reflections was 5150. The SAINT-IRIX package was employed for data reduction and unit cell refinement.<sup>27</sup> All of the reflections were indexed, integrated, and corrected for Lorentz polarization and absorption effects using the program SADABS.<sup>28</sup> The structure was solved using the direct-method procedure and Fourier methods of SIR2004<sup>29</sup> and SHELXL97<sup>30</sup> (the number of parameters was 188). Hydrogen atoms were located by successive Fourier difference maps and refined by isotropic displacement. The agreement factors converged to  $R1 = 0.0461$  and  $wR2 = 0.0828$  for observed reflections and to  $R1 = 0.0798$  and  $wR2 = 0.0950$  for all reflections. Calculations and molecular graphics were performed using the PARST97,<sup>31</sup> WinGX,<sup>32</sup> and ORTEP-3 for Windows<sup>33</sup> packages. Data collection and refinement parameters are summarized in Table 2. The structure solution was complicated by the presence of disorder in the  $\text{cis-1,4-DACH}$  ligand.

(27) SAINT-IRIX; Bruker AXS Inc.: Madison, WI, 2003.

(28) Sheldrick, G. M. *SADABS 2006/1: Program for Empirical Absorption Correction of Area Detector Data*; University of Göttingen, Göttingen, Germany, 2006.

(29) Burla, M. C.; Camalli, M.; Carrozzini, B.; Cascarano, G. L.; Giacovazzo, C.; Polidori, G.; Spagna, R. *J. Appl. Crystallogr.* **2003**, *36*, 1103.

(30) Sheldrick, G. M. *SHELXL-97: Program for the Refinement of Crystal Structures*; University of Göttingen: Göttingen, Germany, 1997.

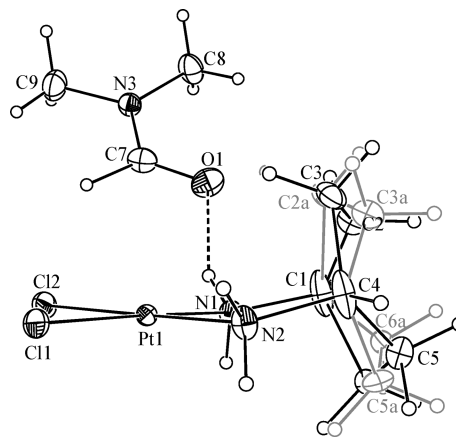
**Table 2.** Crystal Data and Structure Refinement Parameters for [PtCl<sub>2</sub>(*cis*-1,4-DACH)]·DMF

|   |  |
|---|--|
| empirical formula                                   | C <sub>9</sub> H <sub>21</sub> Cl <sub>2</sub> N <sub>3</sub> OPt                                      |
| formula weight                                      | 453.28   |
| temperature   | 293(2) K   |
| wavelength  | 0.71073 Å  |
| crystal system                                      | monoclinic   |
| space group   | <i>P</i> 2 <sub>1</sub> / <i>c</i>   |
| unit cell parameters                                | <i>a</i> = 11.9138(4) Å<br><i>b</i> = 13.2679(4) Å<br><i>c</i> = 9.3672(3) Å<br><i>β</i> = 111.747(2)° |
| <i>V</i>  | 1375.30(8) Å <sup>3</sup>  |
| <i>Z</i>  | 4  |
| <i>D</i> <sub>calcd</sub>                           | 2189 kg/m <sup>3</sup>   |
| <i>μ</i>  | 10.576 mm <sup>-1</sup>  |
| <i>F</i> (000)                                      | 864  |
| crystal size  | 0.400 mm × 0.300 mm × 0.080 mm   |
| <i>θ</i> range                                      | 2.40–33.10°  |
| index ranges  | −18 ≤ <i>h</i> ≤ 18; −19 ≤ <i>k</i> ≤ 20;<br>−14 ≤ <i>l</i> ≤ 13                                       |
| no. of measured reflections                         | 27693  |
| no. of independent reflections                      | 5150 [R(int) = 0.0782]   |
| absorption correction                               | SADABS (Sheldrick, 1996)   |
| refinement method                                   | full-matrix least-squares on <i>F</i> <sup>2</sup>   |
| no. of data points/restraints/parameters            | 5150/0/188   |
| goodness-of-fit on <i>F</i> <sup>2</sup>            | 1.033  |
| final <i>R</i> indices [ <i>I</i> > 2σ( <i>I</i> )] | <i>R</i> 1 = 0.0461, <i>wR</i> 2 = 0.0828  |
| <i>R</i> indices (all data)                         | <i>R</i> 1 = 0.0798, <i>wR</i> 2 = 0.0950  |
| largest diff. peak and hole                         | 3.335 and −2.545 e/Å <sup>3</sup>  |

### 3. Results and Discussion

**3.1. Synthesis and Characterization of [PtCl<sub>2</sub>(*cis*-1,4-DACH)].** To prepare [PtCl<sub>2</sub>(*cis*-1,4-DACH)], we followed the method reported by Khokhar and co-workers<sup>26</sup> with some modifications. The major difficulty encountered in the preparation of this compound arises from the large bite of the *cis*-1,4-DACH ligand, which destabilizes chelation of a single metal center in comparison with bridging two distinct metal ions. In order to overcome this difficulty, we blocked two *cis* coordination positions of platinum with a stable, rather bulky ligand, CBDCA. The intermediate species containing chelated CBDCA, monodentate *cis*-1,4-DACH, and a fourth ligand (dmso in our synthetic procedure) was relatively stable and unreactive and therefore favored intramolecular rearrangement involving coordination of the second donor atom of *cis*-1,4-DACH and displacement of dmso. Once the *cis*-1,4-DACH ligand reaches the chelated form, it is very stable; therefore the CBDCA ligand could be displaced with concentrated hydrochloric acid without affecting the coordination of the diamine. [PtCl<sub>2</sub>(*cis*-1,4-DACH)] was fully characterized by multinuclear NMR spectroscopy (Table 1) and X-ray crystallography.

**3.2. Crystal and Molecular Structure of [PtCl<sub>2</sub>(*cis*-1,4-DACH)]·DMF.** Crystals of [PtCl<sub>2</sub>(*cis*-1,4-DACH)] suitable for X-ray investigation were obtained from a DMF solution layered under Et<sub>2</sub>O and contained one molecule of DMF per molecule of complex. An ORTEP drawing of the complex and the cocrystallized solvent molecule is shown in Figure 2. Selected bond lengths and angles are given in

**Figure 2.** ORTEP drawing of the [PtCl<sub>2</sub>(*cis*-1,4-DACH)]·DMF complex. The ellipsoids enclose 20% probability. *δ* and *λ* puckering of the cyclohexane ring are shown in black and gray, respectively.**Table 3.** Selected Bond Lengths (Å) and Angles (deg) for [PtCl<sub>2</sub>(1,4-DACH)]·DMF

|         |          |             |          |
|---------|----------|-------------|----------|
| Pt1–N1  | 2.056(5) | N1–Pt1–N2   | 96.6(2)  |
| Pt1–N2  | 2.054(5) | N1–Pt1–Cl1  | 177.5(2) |
| Pt1–Cl1 | 2.326(2) | N1–Pt1–Cl2  | 85.2(2)  |
| Pt1–Cl2 | 2.325(2) | N2–Pt1–Cl1  | 85.2(2)  |
| N1–C1   | 1.481(8) | N2–Pt1–Cl2  | 178.1(2) |
| N2–C4   | 1.499(8) | Cl1–Pt1–Cl2 | 93.1(1)  |

Table 3. The Pt atom has a square planar coordination geometry, and the donor atoms are the two nitrogens of *cis*-1,4-DACH and two chloride ions. The largest deviation from the plane defined by the four donor atoms was found for N2 [0.0266(1) Å].

**3.2.1. Bond Distances and Angles within the Coordination Sphere.** The average Pt–ligand bond distances [2.055(5) Å for Pt–N and 2.325(2) Å for Pt–Cl] are in good agreement with values found in structurally related complexes.<sup>34,35</sup> The bond angles between *cis* ligands deviate significantly from the idealized value of 90°. The N–Pt–N angle, which is determined by geometric constraints within the ligand moiety, is particularly large [96.6(2)°]. Although the *cis*-1,4-DACH ligand forms a large seven-membered chelate ring with the platinum atom, because of its cyclic structure it can undergo only a limited amount of puckering. Similar values of the bite angle have been observed previously in other complexes involving *cis*-1,4-DACH, such as [Pt(*cis*-1,4-DACH)(9-methylguanine)<sub>2</sub>]<sup>2+</sup> [97.4(8)°], [Pt(*cis*-1,4-DACH)(1-methylcytosine)<sub>2</sub>]<sup>2+</sup> [97.7(3)°],<sup>17</sup> *cis,trans*-[PtCl<sub>2</sub>(acetate)<sub>2</sub>(*cis*-1,4-DACH)] [97.4(5)°],<sup>7c</sup> *trans*-[PtCl<sub>2</sub>(1,1-cyclobutanedicarboxylate)(*cis*-1,4-DACH)] [98.7(7)°],<sup>7d</sup> [PtCl<sub>4</sub>(*cis*-1,4-DACH)] [98.4(3)°],<sup>7c</sup> and [Pt(malonate)(*cis*-1,4-DACH)] [100.0(2)°].<sup>7b</sup> The strain of the ligand is also apparent from the large Pt–N–C angles [125.2(4) and 124.9(4)° for Pt1–N1–C1 and Pt1–N2–C4, respectively]; these values are greater than those of corresponding angles in other [PtX<sub>2</sub>(1,2-DACH)]

(31) (a) Nardelli, M. *Comput. Chem.* **1983**, 7, 95. (b) Nardelli, M. *J. Appl. Crystallogr.* **1995**, 28, 659.

(32) Farrugia, L. J. *J. Appl. Crystallogr.* **1999**, 32, 837.

(33) Farrugia, L. J. *J. Appl. Crystallogr.* **1997**, 30, 565.

(34) Choi, H.-K.; Hung, S. K.-S.; Bau, R. *Biochem. Biophys. Res. Commun.* **1988**, 156, 1125.

(35) (a) Khokhar, A. R.; Xu, Q.; Al-Baker, S. *J. Inorg. Biochem.* **1993**, 52, 51. (b) Xu, Q.; Khokhar, A. R. *J. Inorg. Biochem.* **1992**, 48, 217.

complexes, which range from 105 to 113°. <sup>35a,36</sup> Narrowing of the N–Pt–Cl angles (average value of 85.2°) compensates for the large N–Pt–N bite angle. This narrowing, however, is greater than expected, since it is also accompanied by a widening of the Cl–Pt–Cl angle [93.1(1)°], which is much larger than the idealized angle of 90°. The most likely explanation for the latter observation is that there is an electrostatic attraction between the electron-deficient aminic protons and the electron-rich chloro ligands accompanied by an electrostatic repulsion between the two electron-rich chloro ligands. Interactions between cis amine and chloro ligands in platinum complexes have been the subject of extensive theoretical investigations. <sup>37</sup>

**3.2.2. Disorder in the *cis*-1,4-DACH Ligand.** The cyclohexane ring has the boat conformation, but the CH–CH<sub>2</sub>–CH<sub>2</sub>–CH moieties are puckered rather than planar. Such puckering (handedness established by the straight line through the two CH<sub>2</sub> carbons and that through the two CH carbons) can be either  $\delta$  or  $\lambda$ . These two puckerings are found in the crystal structure with equal weights and are shown in Figure 2 in black ( $\delta$ ) and gray ( $\lambda$ ).

**3.2.3. Crystal Packing.** In addition to the complex, the asymmetric unit contains one molecule of dimethylformamide. The DMF molecule of crystallization is linked to the Pt complex by a hydrogen bond [N1...O1(*x*, *−y* + 1/2, *z* − 1/2) = 2.992(6) Å, (N1)H1A...O1(*x*, *−y* + 1/2, *z* − 1/2) = 2.141(5) Å, N1–H1A...O1(*x*, *−y* + 1/2, *z* − 1/2) = 157(1)° (Figure 2)]. A view of the molecular packing along the *c* axis is shown in Figure S1 in the Supporting Information.

In the crystal, the complexes form dimeric aggregates having the two platinum units placed face-to-face with the chloro ligands of one unit facing the nitrogen atoms of the other unit. Four interplanar hydrogen bonds link the N and Cl atoms of each dimeric aggregate [N1...Cl1(*−x* + 1, *−y*, *−z* + 1) = 3.456(2) Å, (N1)H1B...Cl1(*−x* + 1, *−y*, *−z* + 1) = 2.592(2) Å, N1–H1B...Cl1(*−x* + 1, *−y*, *−z* + 1) = 161(1)°; N2...Cl2(*−x* + 1, *−y*, *−z* + 1) = 3.526(2) Å, (N2)H2A...Cl2(*−x* + 1, *−y*, *−z* + 1) = 2.734(2) Å, N2–H2A...Cl2(*−x* + 1, *−y*, *−z* + 1) = 147(1)°]. The distance between the two symmetry-related Pt atoms is 3.519(1) Å (for comparison, the sum of the van der Waals radii of the two Pt atoms is 3.4–3.6 Å<sup>38</sup>), and the two platinum subunits are eclipsed, with an average value of 1.6° for the Cl–Pt–Pt–N torsion angle (Figure 3). Adjacent dimeric aggregates are held together by two symmetry-related hydrogen bonds, each involving one aminic proton and one

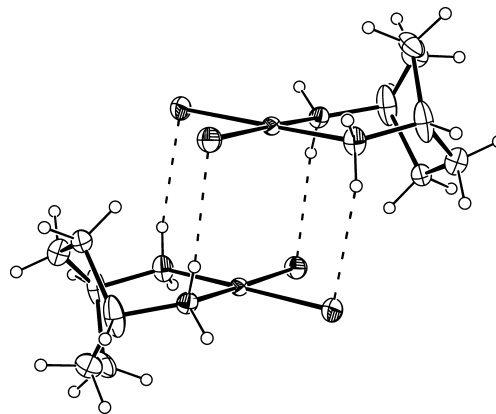


**Figure 3.** ORTEP drawing of a dimeric aggregate consisting of two [PtCl<sub>2</sub>(1,4-DACH)] complexes linked by hydrogen bonds. The aggregate has N...Cl distances in the range 3.45–3.52 Å, (N)H...Cl distances in the range 2.59–2.73 Å, and N–H...Cl angles in the range 147–161°.

**Table 4.** <sup>1</sup>H Chemical Shifts (ppm) of (*cis*-1,4-DACH)PtG<sub>2</sub> Adducts in D<sub>2</sub>O Solution at Ambient Temperature

| compound                                       | pH*  | H8   | H1'  | H <sub>a</sub> | H <sub>b</sub> |
|--|------|------|------|----------------|----------------|
| ( <i>cis</i> -1,4-DACH)Pt(3'-GMP) <sub>2</sub> | 3.06 | 8.39 | 5.91 | 3.37           | 1.79–1.97      |
| ( <i>cis</i> -1,4-DACH)Pt(5'-GMP) <sub>2</sub> | 3.29 | 8.34 | 5.86 | 3.35           | 1.75–1.94      |

chloro ligand [N2...Cl1(*x*, *−y* + 1/2, *z* + 1/2) = 3.564(3) Å, (N2)H2B...Cl1(*x*, *−y* + 1/2, *z* + 1/2) = 2.894(1) Å, N2–H2B...Cl1(*x*, *−y* + 1/2, *z* + 1/2) = 132(1)°], forming a chain extending along the *b* direction. The crucial role of hydrogen bonds in this type of compound has already been addressed. <sup>39</sup>

**3.3. Reaction with G Nucleotides.** In order to prepare (*cis*-1,4-DACH)PtG<sub>2</sub> adducts, we first converted the dichloro species into the more soluble and reactive aqua-sulfato species. This latter compound was placed in an NMR tube and allowed to react with G bases in acidic D<sub>2</sub>O.

**3.3.1. 3'-GMP.** The <sup>1</sup>H NMR spectrum of a solution containing [Pt(OSO<sub>3</sub>)(*cis*-1,4-DACH)(OH<sub>2</sub>)] and 3'-GMP (with a molar ratio of 1:2 at pH\* 3.06) taken soon after mixing of the reagents (see Figure S2a in the Supporting Information) exhibited two main signals in the range typical for H8 peaks: the signals at 8.15 and 8.39 ppm were assigned to H8 in free 3'-GMP and the bis adduct, respectively (Table 4). In addition, a very weak signal at 8.56 ppm was assigned to H8 of the monoadduct on the basis of literature data. In the region of *cis*-1,4-DACH protons, the singlet at 3.37 ppm was assigned to H<sub>a</sub> (see Table 1 for labeling of the protons), and the signal at 1.79–1.97 ppm was assigned to H<sub>b</sub> (Table 4). The very weak signals at 3.05 and 1.79 ppm were assigned to H<sub>a</sub> and H<sub>b</sub> protons, respectively, of the reactant aqua complex. The <sup>1</sup>H NMR spectrum recorded after a reaction time of 2 days (see Figure S2b in the Supporting Information) exhibited only the signals belonging to the bis adduct, indicating that the reaction had reached completion. Only one set of G signals was observed for the bis adduct, indicating that interconversion between possible conformers at the ambient temperature was fast on the NMR time scale.

Under these circumstances, it is possible to detect which conformer is dominant in solution using CD spectroscopy.

(36) (a) Abu-Surrah, A. S.; Al-Allaf, T. A. K.; Klinga, M.; Ahlgren, M. *Polyhedron* **2003**, *22*, 1529. (b) Al-Allaf, T. A. K.; Rashan, L. J.; Steinborn, D.; Merzweiler, K.; Wagner, C. *Transition Met. Chem.* **2003**, *6*, 717. (c) Bruck, M. A.; Bau, R.; Noji, M.; Inagaki, K.; Kidani, Y. *Inorg. Chim. Acta* **1984**, *92*, 297. (d) Carland, M.; Tan, K. J.; White, J. M.; Stephenson, J.; Murray, V.; Denny, W. A.; McFadyen, W. D. *J. Inorg. Biochem.* **2005**, *99*, 1738. (e) Fails, T. W.; Hall, M. D.; Hambley, T. W. *Dalton Trans.* **2003**, 1596. (f) Khokhar, A. R.; Xu, Q.; Al-Baker, S.; Lumetta, G. J. *Inorg. Chim. Acta* **1993**, *203*, 121. (g) Lee, Y.-A.; Chung, Y. K.; Sohn, Y. S. *Inorg. Chim. Acta* **1999**, *295*, 214.

(37) Carloni, P.; Andreoni, W.; Hutter, J.; Curioni, A.; Giannozzi, P.; Parrinello, M. *Chem. Phys. Lett.* **1995**, *234*, 50.

(38) Bondi, A. *J. Phys. Chem.* **1964**, *68*, 441.

(39) Reedijk, J. *Inorg. Chim. Acta* **1992**, *198–200*, 873.



The CD spectrum of the solution of (*cis*-1,4-DACH)Pt(3'-GMP)<sub>2</sub> at pH 3.0 showed two negative Cotton features (at 227 and 293 nm) and two positive Cotton features (at 208 and 253 nm). On the basis of previous studies reported by the groups of Natile and Marzilli,<sup>16</sup> the CD spectrum is indicative of the chirality ( $\Delta$  or  $\Lambda$ ) of the dominant HT conformer in solution. In the present case, the shape of the CD spectrum was typical of a  $\Delta$ HT conformer, indicating that the  $\Delta$ HT conformer is dominant over the  $\Lambda$ HT conformer in solution.

The CD spectrum was also recorded at different pH values. Increasing the pH from 3.0 to 7.1 caused the intensities of the CD signals to increase. However, an additional increase in pH from 7.1 to 11.0 caused the intensities of the CD signals to decrease; at pH  $\geq 10$ , the intensities of the low-energy bands (253 and 293 nm) fell practically to zero. This behavior agreed with previous findings suggesting that the  $\Delta$ HT conformation of the two *cis* 3'-GMP ligands is stabilized by a H-bonding interaction between the phosphate group of one nucleotide and the N1H group of the other. Such an interaction is greatest (largest Cotton effect) at pH  $\sim 7$ , where the phosphate group is completely deprotonated while the N1H group has not yet started to deprotonate. The occurrence of such an internucleotide interaction is also supported by molecular models of *cis*-A<sub>2</sub>Pt(3'-GMP)<sub>2</sub> complexes,<sup>40</sup> which show that the phosphate group of one 3'-GMP can reach over the N1H group of the other 3'-GMP in the  $\Delta$ HT conformation, assuming that the nucleotides maintain the usual anti conformation.

**3.3.2. 5'-GMP.** The <sup>1</sup>H NMR spectrum of a solution containing [Pt(OSO<sub>3</sub>)(*cis*-1,4-DACH)(OH<sub>2</sub>)] and 5'-GMP (in a molar ratio of 1:2 at pH\* 3.29) taken soon after mixing of the reagents (see Figure S3a in the Supporting Information) showed two main signals in the range typical for H8 protons: the signals at 8.34 and 8.24 ppm were assigned to H8 in the bis-adduct and unreacted 5'-GMP, respectively (Table 4). In the region of *cis*-1,4-DACH protons, the singlet at 3.35 ppm was assigned to H<sub>a</sub>, and the broad multiplet in the range 1.75–1.94 ppm was assigned to H<sub>b</sub>. In the same region, very weak signals at 3.0 and 1.7 ppm belonging to the reactant Pt complex could also be observed. After a reaction time of 6 days, the peaks of the starting reagents had disappeared completely, and the <sup>1</sup>H NMR spectrum (see Figure S3b in the Supporting Information) exhibited only the signals belonging to the bis adduct (*cis*-1,4-DACH)Pt(5'-GMP)<sub>2</sub>. As in the case of 3'-GMP, only one set of signals for the bis adduct was observed in the NMR spectrum, indicating that interconversion between possible conformers at the ambient temperature was fast on the NMR time scale.

The CD spectrum recorded on a sample taken from the NMR solution (diluted as described in Section 2.3) showed two positive Cotton effects (at 225 and 286 nm) and two negative Cotton effects (at 203 and 252 nm) (Figure 4, pH 7.2). There was an inversion in the signs of the Cotton effects in going from the 3'-GMP to the 5'-GMP complex, indicating

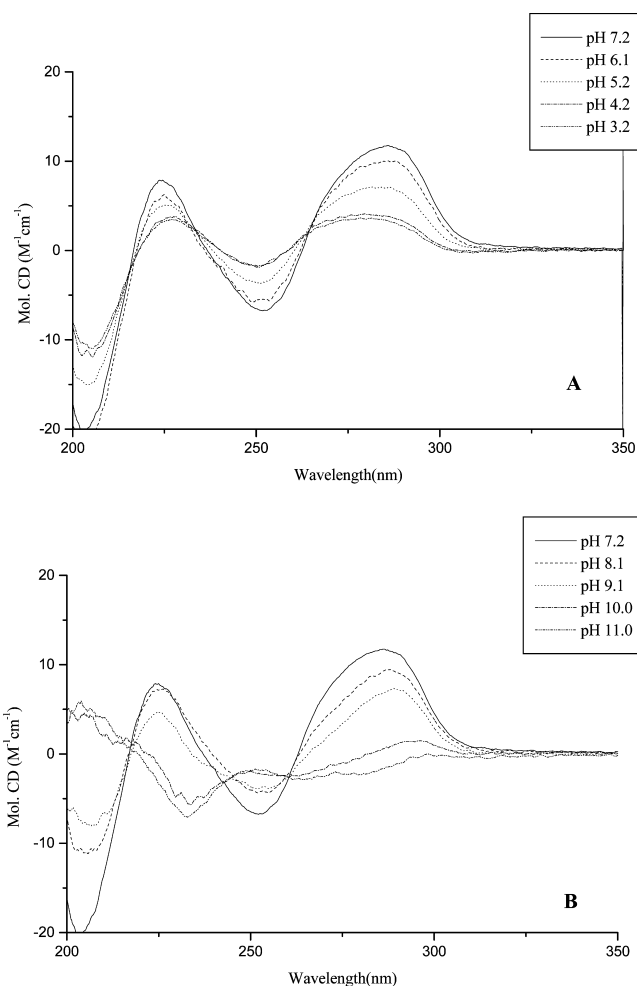


**Figure 4.** CD spectra of (*cis*-1,4-DACH)Pt(5'-GMP)<sub>2</sub> in solution: (A) pH 7.2–3.2; (B) pH 7.2–11.0.

that in the latter case, the dominant HT conformer has  $\Lambda$  chirality. This result was in full agreement with previous observations indicating that stabilization stemming from interactions between the 5'-phosphate group of one G and the N1H group of the other are possible only for the  $\Lambda$ HT conformer (the 5'-phosphates protrude toward the *cis* G, assuming that the nucleotides keep the usual anti conformation).

As in the case of 3'-GMP, the CD spectra were recorded at different pH values. The intensities of the CD signals increased as the pH increased from 3.2 to 7.2 (Figure 4A). In contrast, a subsequent increase of the pH from 7.2 to 11.0 resulted in a decrease in intensity of the CD signals (Figure 4B); at pH  $\geq 10$ , the intensities of the low-energy bands (252 and 286 nm) fell practically to zero. Therefore, the highest intensity of the CD signals was reached at neutral pH, where the 5'-phosphate group is completely deprotonated while the N1H group has not yet undergone deprotonation.

Comparison of the intensities of the CD signals (e.g., the Cotton feature at 290 nm for pH  $\sim 7$ ) for the series of *cis*-A<sub>2</sub>Pt(5'-GMP)<sub>2</sub> complexes with A<sub>2</sub> = en, (NH<sub>3</sub>)<sub>2</sub>, pn, and (*cis*-1,4-DACH) showed that the intensity increased as the bite angle of the A<sub>2</sub> ligand(s) increased. An analogous trend was observed for the 3'-GMP complexes.

(40) Wong, H. C.; Shinozuka, K.; Natile, G.; Marzilli, L. G. *Inorg. Chim. Acta* **2000**, *297*, 36.

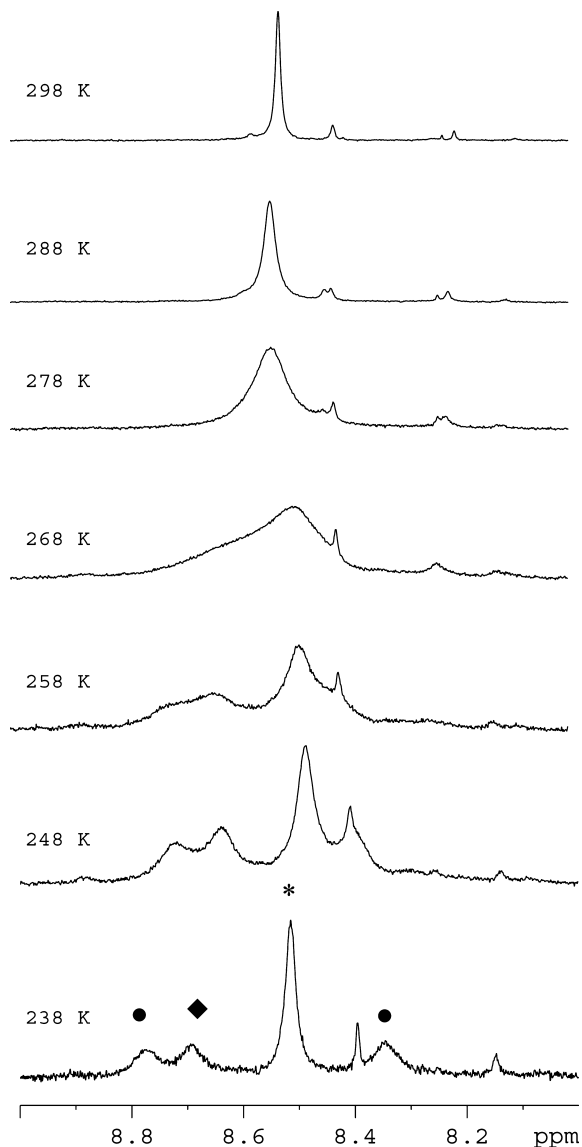


**Figure 5.**  $^1\text{H}$  NMR (600 MHz) spectra in the region of H8 resonances for the bis-adduct  $(\text{cis-1,4-DACH})\text{Pt}(5'\text{-GMP})_2$  in 2:1 (v/v)  $\text{D}_2\text{O}/\text{CD}_3\text{OD}$  ( $\text{pH}^* 5.83$ ) at different temperatures. The two signals marked with • belong to the HH conformer, while the signals marked with \* and ◆ belong to the  $\Delta\text{HT}$  and  $\Delta\text{HT}$  conformers, respectively. The remaining signals are due to impurities.

**3.4. Slowing the Rate of Interconversion between Conformers in  $(\text{cis-1,4-DACH})\text{Pt}(5'\text{-GMP})_2$  by Decreasing the Temperature.** We have already pointed out that, notwithstanding the large bite angle of the *cis*-1,4-DACH carrier ligand, interconversion between conformers of  $(\text{cis-1,4-DACH})\text{Pt}(\text{GMP})_2$  complexes at room temperature is still fast on the NMR time scale, as in the case of cisplatin and analogous compounds with primary chelating diamines (en, 1,2-DACH, and pn). However, we hypothesized that the rate of interconversion between conformers could be decreased by decreasing the temperature. Therefore, we dissolved a sample of  $(\text{cis-1,4-DACH})\text{Pt}(5'\text{-GMP})_2$  in 2:1 (v/v)  $\text{D}_2\text{O}/\text{CD}_3\text{OD}$  ( $\text{pH}^* 5.83$ ) and recorded  $^1\text{H}$  NMR spectra over the temperature range 298–238 K (Figure 5). Generally, the G H8 NMR signal alone can be used to identify conformers, since it is located in an isolated region of the spectrum and exhibits the greatest dependence on conformation. Moreover,

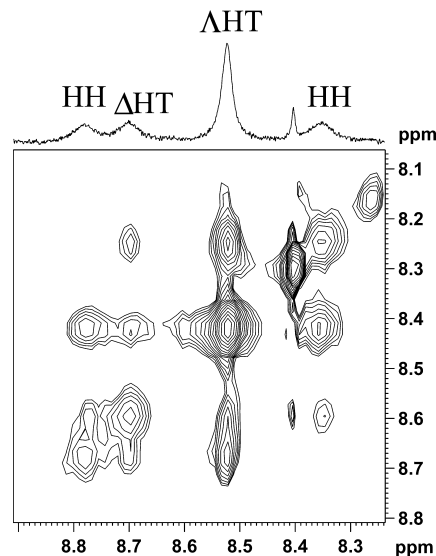


**Figure 6.** (top)  $^1\text{H}$  NMR spectrum and (bottom) 2D-ROESY (600 MHz) contour map recorded on a sample of  $(\text{cis-1,4-DACH})\text{Pt}(5'\text{-GMP})_2$  in 2:1 (v/v)  $\text{D}_2\text{O}/\text{CD}_3\text{OD}$  ( $\text{pH}^* 5.83$ ) at 238 K. The cross-peaks are in phase with respect to the diagonal peaks, indicating that the cross-peaks are exchange peaks rather than through-space correlations).

for *cis*- $\text{A}_2\text{PtG}_2$  complexes with  $\text{A}_2$  ligand(s) having  $C_2$  symmetry and G's containing asymmetric sugar residues, up to four  $^1\text{H}$  NMR signals can be observed [one for each HT form ( $\Delta$  and  $\Delta$ ) and two signals of equal intensity for the HH form]. Decreasing the temperature caused the single H8 NMR signal observed at 298 K to decoalesce into four signals assignable to the three possible conformers. Warming the NMR sample back to room temperature restored the initial spectrum, confirming the presence of a dynamic equilibrium.

In order to assign the four H8 peaks detected at 238 K to the corresponding conformers, a rotating-frame nuclear Overhauser effect (NOE) spectroscopy (ROESY) experiment was performed at low temperature (Figure 6). Our intention was to detect a cross-peak between the H8 signals of the HH conformer, in which the two H8 protons are on the same side of the platinum coordination plane at a distance compatible with NOESY and ROESY experiments.<sup>16</sup> Unfortunately, even at 238 K, the cross-peaks observed in the ROESY experiment appeared to be exchange peaks (i.e., in phase with the diagonal peaks) rather than spatial couplings between protons. However, since rotation of a single guanine converts the HH conformer into an HT conformer and vice versa, it follows that the two H8's of the HH conformer can exchange only with the H8's of the HT conformers and not with themselves. Therefore, the only exchange cross peak missing in the ROESY spectrum should be the one between the two signals of the HH conformer. The two signals falling at 8.78 and 8.35 ppm (Figure 6) were the only ones lacking cross-peaks, and they were therefore assigned to the HH conformer. In order to unambiguously assign the remaining H8 signals to the  $\Delta\text{HT}$  and  $\Delta\text{HT}$  conformers, we considered the relative abundance of the two HT rotamers, as indicated by the CD spectrum. The CD spectrum clearly showed that  $\Delta\text{HT}$  was the dominant conformer, and therefore, the more-intense HT signal at 8.52 ppm (the intensities of the two



HT signals were 51 and 16% of the total) was assigned to the AHT conformer.

### 3.5. Comparison with the Case of Bulky A<sub>2</sub> Ligands.

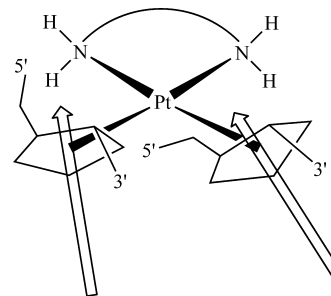
As pointed out in the Introduction, bulky A<sub>2</sub> ligands slow the rotation of the G's around the Pt–N7 bonds in *cis*-A<sub>2</sub>PtG<sub>2</sub> compounds, making observation of different conformers (HT and HH) by NMR spectroscopy possible.<sup>41</sup> Restricted rotation was observed for *cis*-A<sub>2</sub>PtG<sub>2</sub> models containing secondary amine ligands such as *N,N'*-dimethyl-2,3-diaminobutane (Me<sub>2</sub>DAB)<sup>42</sup> and 2,2'-bipiperidine (Bip);<sup>43</sup> tertiary amines such as *N,N,N',N'*-tetramethylethylenediamine (Me<sub>4</sub>en),<sup>13b</sup> *N,N,N',N'*-tetramethyl-1,2-diaminocyclohexane (Me<sub>4</sub>-1,2-DACH),<sup>13a</sup> and *N,N'*-dimethylpiperazine (Me<sub>2</sub>ppz);<sup>41</sup> and heterocyclic N-donor ligands such as 1,10-phenanthroline (phen) and 2,9-dimethyl-1,10-phenanthroline (Me<sub>2</sub>phen).<sup>44</sup> As intended by design, these carrier ligands (Me<sub>2</sub>DAB, Bip, Me<sub>4</sub>en, Me<sub>4</sub>-1,2-DACH, Me<sub>2</sub>ppz, Me<sub>2</sub>phen, and phen) successfully hindered G base rotation in their respective *cis*-A<sub>2</sub>PtG<sub>2</sub> models relative to models with less bulky carrier ligands. However, the extents to which they slow the rotation differed markedly. For example, whereas exchange spectroscopy cross-peaks were observed for (Me<sub>2</sub>-DAB)Pt(5'-GMP)<sub>2</sub> at 5 °C, no such cross-peaks between rotamers of (Me<sub>2</sub>ppz)Pt(1-Me-5'-GMP)<sub>2</sub> were observed at this temperature. Also, saturation transfer was observed between H8 signals of (Me<sub>2</sub>ppz)Pt(5'-GMP)<sub>2</sub> at 25 and 35 °C, but no such transfer of magnetization was observed between the H8 signals of (Bip)Pt(5'-GMP)<sub>2</sub> conformers, even at temperatures up to 80 °C.

The H8 NMR signals of the HH form in *cis*-A<sub>2</sub>PtG<sub>2</sub> complexes involving the secondary diamines Me<sub>2</sub>DAB and Bip were well-separated by ~1 ppm and positioned on either side of the two HT H8 NMR signals. In contrast, the two H8 NMR signals of the HH rotamer for the complexes involving the tertiary diamines Me<sub>4</sub>en, Me<sub>4</sub>-1,2-DACH, and Me<sub>2</sub>ppz were both downfield from the HT H8 signals and exhibited a much smaller separation (~0.05–0.13 ppm). Analogous behavior was observed in adducts with phen and Me<sub>2</sub>phen.

The ~1 ppm H8 shift separation commonly observed for the H8 signals of the HH rotamer of adducts with secondary diamines was proposed to stem, at least in part, from relative canting of the two G's. The 6-out canting of one G places its H8 atom closer to the anisotropic ring shielding effect of the *cis* G.

In *cis*-A<sub>2</sub>PtG<sub>2</sub> complexes, canting of the G bases may be influenced by the interaction of G O6 with the carrier ligand (Scheme 2). Low-energy HH structures generated for [(Me<sub>2</sub>-DAB)Pt(9-EtG)<sub>2</sub>]<sup>2+</sup> exhibited one G canted such that its H8 and O6 atoms were closer to the five-membered ring of the adjacent base and the NH of the *cis* amine, respectively,

**Scheme 2.** Schematic Representation of a *cis*-A<sub>2</sub>PtG<sub>2</sub> HH Conformer, in Which Each G Base Is Represented by an Arrow (Whose Tip Points toward H8) and a Sketch of the Ribose<sup>a</sup>



<sup>a</sup> In this scheme, the base on the left is uncanted or has 6-in canting, which allows the phosphate group to H bond with the *cis* amine, whereas the base on the right has 6-out canting, which allows the O6 atom to H bond with NH of the carrier-ligand.

while the other G was uncanted (with its O6 atom on the side of the Me substituent of the *cis* amine). The anisotropic effects of the guanine bases on the H8 shifts were estimated for this [(Me<sub>2</sub>DAB)Pt(9-EtG)<sub>2</sub>]<sup>2+</sup> HH model, and the canted and uncanted G's were calculated to experience shielding and deshielding effects, respectively.

It has been proposed that the much smaller separation (0.1 ppm) commonly observed for the H8 signals of the HH conformer in adducts with tertiary diamines (Me<sub>4</sub>en, Me<sub>4</sub>-1,2-DACH, and Me<sub>2</sub>ppz) or N-donor heterocycles (phen and Me<sub>2</sub>phen) is related to uncanted G's. For instance, the lowest-energy HH conformer structure for [(Me<sub>2</sub>ppz)Pt(9-EtG)<sub>2</sub>]<sup>2+</sup> had both G's oriented almost exactly perpendicular to the platinum coordination plane.<sup>41</sup> Both H8 atoms of the [(Me<sub>2</sub>ppz)Pt(9-EtG)<sub>2</sub>]<sup>2+</sup> HH model were calculated to experience a similar slight deshielding (~0.02 ppm). Consequently, the H8 shifts would be similar, as observed, but unlike those in HH conformers of more typical *cis*-A<sub>2</sub>PtG<sub>2</sub> adducts, where A<sub>2</sub> contains NH groups.

In summary, adducts containing secondary diamines having C<sub>2</sub> symmetry are characterized by a large separation for the H8 signals of the HH conformer because the presence of an amine substituent on the side of the six-membered ring of only one nucleotide imposes a different canting to the two guanines, resulting in very different shifts of the H8 signals. In contrast, adducts with tertiary diamines or with N-donor heterocycles greatly reduce the possibility of canting of both guanines, with the consequence that the two H8 signals have similar chemical shifts. The case of primary diamines such as the *cis*-1,4-DACH ligand investigated in the present work has none of the restrictions of the previously described carrier ligands and will be discussed in detail in Section 3.6.

**3.6. The Case of *cis*-1,4-DACH.** The separation between the two H8 signals of the HH conformer was found to be 0.43 ppm for the (*cis*-1,4-DACH)Pt(5'-GMP)<sub>2</sub> complex. This value is halfway between the values of 1 ppm observed in adducts with secondary diamines and 0.1 ppm observed in adducts with tertiary diamines or N-donor heterocycles. Since the 1,4-DACH ligand has primary amines at both ends and their aminic protons are oriented symmetrically with respect to the platinum coordination plane, it is neutral with respect

(41) Sullivan, S. T.; Ciccarese, A.; Fanizzi, F. P.; Marzilli, L. G. *Inorg. Chem.* **2001**, *40*, 455.

(42) Marzilli, L. G.; Intini, F. P.; Kiser, D.; Wong, H. C.; Ano, S. O.; Marzilli, P. A.; Natile, G. *Inorg. Chem.* **1998**, *37*, 6898.

(43) Ano, S. O.; Intini, F. P.; Natile, G.; Marzilli, L. G. *Inorg. Chem.* **1999**, *38*, 2989.

(44) Margiotta, N.; Papadia, P.; Fanizzi, F. P.; Natile, G. *Eur. J. Inorg. Chem.* **2003**, 1136.

to the different cantings of the two guanines in the HH conformer, which will be entirely determined by the different arrangements of the sugar–phosphate substituents. Assuming an anti conformation for each nucleotide, the 5′-phosphate of one nucleotide will be directed toward the cis amine and that of the other nucleotide toward the cis nucleotide. The former G would be expected to be less canted or uncanted (because of possible H bonding between the 5′-phosphate and the cis amine) and could give the low-field signal, while the latter G would be expected to be more canted (as a result of possible H bonding between the G O6 and the cis amine) and could give the upfield signal.

The assignment of the low-field H8 signal to the G having its phosphate directed toward the cis amine is also supported by the fact that it appears very close to the H8 signal of the  $\Delta$ HT rotamer, in which both G's have their 5′-phosphate groups directed toward the cis amines. Similarly, the assignment of the high-field H8 signal to the G having its phosphate directed toward the cis G is supported by the fact that it is located quite close to the H8 signal of the  $\Delta$ HT rotamer, in which both G's have their 5′-phosphate groups directed toward the cis G. The appearance of one HH H8 signal at a lower field with respect to the  $\Delta$ HT H8 signal does not necessarily imply a greater 6-in canting of this G, since this signal location could be a consequence merely of the smaller shielding provided by the adjacent G, which has H8 instead of the six-membered ring on the same side of the platinum coordination plane. On the other hand, we believe that the greater shielding of the other HH H8 signal with respect to the  $\Delta$ HT H8 signal is an indication of significant 6-out canting of this G in contrast to the two bases in  $\Delta$ HT, which can be uncanted or even have 6-in canting.

It is interesting to note that separations of this order of magnitude have been observed in adducts of cisplatin and related compounds with short oligonucleotides, with the H8 signal of the 5′-G always appearing at lower field (e.g., 8.742 vs 8.159 in a dodecamer duplex,<sup>45</sup> 8.66 vs 8.39 in a 9-mer duplex,<sup>46</sup> and 8.76 vs 8.19 in an 8-mer duplex<sup>47</sup>). Therefore, it can be concluded that while model compounds containing secondary diamines gave far too great a separation between the H8 signals of the HH conformer [e.g., 8.94 vs 8.02 in ((S,R,R,S)-Me<sub>2</sub>DAB)Pt(5′-GMP)<sub>2</sub>]<sup>42</sup> and model compounds containing tertiary amines or N-donor heterocycles far too small a separation [e.g., 8.59 vs 8.54 ppm in (Me<sub>4</sub>en)Pt(5′-GMP)<sub>2</sub>]<sup>13a</sup>], the model compound containing the primary diamine (*cis*-1,4-DACH)Pt(5′-GMP)<sub>2</sub> gives H8 chemical shift values in good agreement with those of actual intrastrand cisplatin-cross-linked DNA duplexes.

In order to correlate our findings with published data for intrastrand cisplatin-cross-linked DNA duplexes, we performed a *gedanken* experiment on the (*cis*-1,4-DACH)Pt(5′-GMP)<sub>2</sub> HH model, in which the guanosine with the 5′-phosphate directed toward the cis G was linked to the 3′-

hydroxyl group of the cis G. In the resulting pGpG dinucleotide, the former guanine occupied the 3′ position and the latter the 5′ position. This established a relationship between guanines of untethered *cis*-A<sub>2</sub>Pt(5′-GMP)<sub>2</sub> HH models and those of adducts with tethered guanines: the guanine with the phosphate directed toward the cis amine corresponded to a “5′-G”, while the guanine with the 5′-phosphate directed toward the cis G corresponded to a “3′-G”. According to the previous assignment, the “5′-G” H8 was found at lower field while the “3′-G” H8 was found at higher field. This is exactly what is normally found in cross-links of cisplatin with double-stranded oligonucleotides for which the HH orientation of the cross-linked guanines is firmly established.

It should be noted that this is not the case for cis-G cross-links of single-stranded oligodeoxynucleotides, for which the 5′-G H8 is generally found at higher field than the 3′-G H8.<sup>48</sup> In fact, in Pt adducts with single-stranded oligodeoxynucleotides, the signal for the H8 of the 5′-G involved in the 1,2-intrastrand cross-link falls at 8.0 ppm while that for the 3′-G H8 falls at 9.0 ppm (giving a value of  $\Delta\delta$  between the two H8's of 1.0 ppm in most of the cases).<sup>49</sup> We believe that this is due to the flexible structure of cross-linked single-stranded oligonucleotides, which allows contributions to arise from different conformers as well as from wrapping of the oligonucleotide around the metal cation. It is worth mentioning that downfield 5′-G and upfield 3′-G signals, such as those found in the present investigation and in cross-links of cisplatin with double-stranded oligonucleotides, were also found in the adduct of cisplatin with the ribonucleotide r(GpG).<sup>49</sup>

#### 4. Conclusions

The results obtained with (*cis*-1,4-DACH)Pt adducts of 3′-GMP and 5′-GMP agree with those from previous work in our laboratories. In particular, (*cis*-1,4-DACH)Pt(3′-GMP)<sub>2</sub> has a preference for the  $\Delta$ HT conformation, while the (*cis*-1,4-DACH)Pt(5′-GMP)<sub>2</sub> has a preference for the  $\Delta$ HT conformation. In both cases, the Cotton effects are largest at neutral pH, where the phosphate group is completely deprotonated while the N1H has not yet started to undergo deprotonation.

An important point has emerged from comparison of the intensities of the CD signals for the series of *cis*-A<sub>2</sub>Pt(5′-GMP) complexes with A<sub>2</sub> = en, (NH<sub>3</sub>)<sub>2</sub>, pn, and *cis*-1,4-DACH. The intensities of the Cotton effects increase as the bite angle of the A<sub>2</sub> ligand(s) increases. The increase in Cotton-effect intensities could have different explanations. The most straightforward explanation is that increasing the bite angle of the A<sub>2</sub> ligand(s) increases the phosphate–cis-G N1H internucleotide interaction and therefore the percentage of the dominant  $\Lambda$  conformer as well. Support for this hypothesis comes from the observation that the dihedral angle between the two 5′-GMP's in the single  $\Delta$ HT conformer so

(45) Gelasco, A.; Lippard, S. J. *Biochemistry* **1998**, *37*, 9230.

(46) Marzilli, L. G.; Saad, J. S.; Kuklenyik, Z.; Keating, K. A.; Xu, Y. *J. Am. Chem. Soc.* **2001**, *123*, 2764.

(47) Yang, D.; van Boom, S. S. G. E.; Reedijk, J.; van Boom, J. H.; Wang, A. H.-J. *Biochemistry* **1995**, *34*, 12912.

(48) Marcelis, A. T. M.; Den Hartog, J. H. J.; Van Der Marel, G. A.; Wille, G.; Reedijk, I. *Eur. J. Biochem.* **1983**, *135*, 343.

(49) Kozelka, J.; Fouchet, M.-H.; Chottard, J.-C. *Eur. J. Biochem.* **1992**, *205*, 895 and references therein.

far reported is very narrow  $[44.2(2)^\circ]^{13b}$  and hence could be favored by a large bite of the carrier ligand(s). However, the intensity of the Cotton effect also depends upon the canting of the two nucleobases with respect to the coordination plane (in an HT conformer, the two G's have identical canting). The greatest Cotton effect is expected for nucleobases orthogonal to the coordination plane and a Cotton effect close to zero for nucleobases lying in the coordination plane. It is therefore also possible that the greater intensity of the Cotton effect in the *cis*-1,4-DACH complex compared with those for the en,  $(\text{NH}_3)_2$ , and pn derivatives could be due to smaller canting of the nucleobases rather than an increase in the percentage of the dominant conformer.

The  $^1\text{H}$  NMR experiments performed at low temperature have shown for the first time in *cis*- $\text{A}_2\text{PtG}_2$  complexes with primary diamines or two *cis*-ammines the decoalescence of the single H8 NMR signal observed at room temperature into four signals arising from the three possible conformers HH,  $\Delta\text{HT}$ , and  $\Delta\text{HT}$ . The mixture of these three conformers was in dynamic equilibrium with a composition of 33, 51, and 16%, respectively. This result is of great significance since it is the first to provide an indication of the relative abundance of different conformers in a system very similar to cisplatin, the clinically relevant drug. We emphasize that no X-ray structures of *cis*-nucleotide HH conformers have been published to date; furthermore, while solution CD investigations performed on cisplatin or model compounds with primary diamines have provided evidence for the dominance of one HT conformer over the other, they have been totally unable to give an estimate of the relative abundance of the three possible conformers for a system containing untethered nucleotides (although CD investigations have given estimates of the relative abundance of different conformers in cisplatin adducts with tethered nucleotides, such as  $\text{GpG}^{50}$ ). This work represents the first

case of such an estimate and has revealed that even with untethered nucleotides, the HH conformer can account for one-third of the total. Moreover, the H8 chemical shifts of this identified single HH conformer are very close to those normally observed in cross-links of cisplatin with double-stranded oligonucleotides for which the HH orientation of the cross-linked guanines is determined by the pairing of the two strands.

We hope that the *cis*-1,4-DACH carrier ligand will also prove to be useful in investigating different conformers of adducts with single- and double-stranded oligonucleotides, as a further step in the elucidation of the different anticancer activity of  $[\text{PtCl}_2(1,4\text{-DACH})]$  as compared with cisplatin and oxaliplatin. This appears to be crucial, since the antitumor activity is mediated by a number of cellular proteins [mismatch-repair and damage-recognition proteins such as high-mobility group box protein 1 (HMGB1), TATA box-binding protein, and human upstream binding factor]<sup>8</sup> that specifically recognize DNA adducts formed by platinum-based drugs.

**Acknowledgment.** We are grateful to Prof. Ferdinando Scordari and Dr. Ernesto Mesto (University of Bari) for X-ray crystallography data collection. The authors thank the University of Bari, the Italian “Ministero dell’Istruzione, Università e Ricerca (MUR)” (PRIN 2005 n. 2005032730\_001), and the EC (COST Chemistry project D39/0004/06) for support.

**Supporting Information Available:** Crystallographic data for  $[\text{PtCl}_2(\textit{cis}\text{-}1,4\text{-DACH})]\cdot\text{DMF}$  in CIF format, a figure showing the molecular packing along the *c* axis in  $[\text{PtCl}_2(\textit{cis}\text{-}1,4\text{-DACH})]\cdot\text{DMF}$ , and  $^1\text{H}$  NMR spectra used for monitoring the reactions of  $[\text{Pt}(\text{OSO}_3)(\textit{cis}\text{-}1,4\text{-DACH})(\text{OH}_2)]$  with 3'-GMP and 5'-GMP in  $\text{D}_2\text{O}$ . This material is available free of charge via the Internet at <http://pubs.acs.org>.

IC702202X

(50) Williams, K. M.; Cerasino, L.; Natile, G.; Marzilli, L. G. *J. Am. Chem. Soc.* **2000**, *122*, 8021.